Somatic *STAT5B*^{N642H} mutations shape variable immune landscapes resulting in heterogenous immune diseases

Sarah Grün, MSc,[a,b,c] Anne Rensing-Ehl, MD,[a] Tobias Suske, PhD,[d] Julian Wolter-Mess, PhD,[b,c,e] Jonathan Gehrig, MSc,[a,b] Jasmin Mann, MSc,[a,b] Christoph König, MSc,[a,b] Mathias Hauri, MD, PhD,[f] Maximilian Heeg, MD,[a,g] Timothy Ronan Leahy, MD,[h] David Genevieve, MD, PhD,[i] Jean-Baptiste Gaillard, PharmD,[j] Martin Broly, MD,[k] Arnaud Bourdin, MD, PhD,[l] Carla Castro, PhD,[a] Lea Seidel, MSc,[b,m] Bertram Bengsch, MD, PhD,[c,m] Peter Aichele, PhD,[a] Kristoffer Weißert, PhD,[a] Juncal Fernandez-Orth, PhD,[n] Vincent Schipperges, PhD,[o] Geoffroy Andrieux, PhD,[o] Melanie Boerries, MD, PhD,[o,p] Nina Cabezas-Wallscheid, PhD,[c,e] Miriam Erlacher, MD, PhD,[g,q] Roland Elling, MD,[g] Carsten Speckmann, MD,[a,g] Lara Heller, PhD,[r,s] Björn Schulte, PhD,[r,s] Myriam Lorenz, PhD,[t] Klaus Schwarz, MD,[t,u] Richard Moriggl, MD,[v] and Stephan Ehl, MD[a,c]

Dublin, Ireland; Freiburg, Tübingen, and Ulm, Germany; Montpellier, France; Salzburg and Vienna, Austria; and Zurich, Switzerland

Background: Inborn errors of immunity are traditionally understood as monogenic germline disorders. However, somatic mosaicism can also result in immune-mediated diseases, mimicking inborn errors of immunity. While early postzygotic mosaicism is the predominant mechanism, genetic variants causing a selective advantage to hematopoietic progenitors and/or mature immune cells may cause immune dysregulation and initiate disease at any age. Somatic mosaicism for *STAT5B*^{N642H} was linked to severe allergic disease in infancy, but its full clinical spectrum and underlying mechanisms remain incompletely defined.

Objective: We elucidated how somatic *N642H* mutations of the *STAT5B* gene shape lineage-specific mosaicism, immune cell function, and clinical phenotypes.

Methods: We investigated 3 new patients—including one adult—with *STAT5B*^{N642H} mosaicism using deep sequencing, flow and mass cytometry, and functional immune assays. Mutant cell distribution was mapped across blood lineages. A mouse model with mosaic *STAT5B*^{N642H} mutation in hematopoietic stem cells was generated to study clonal dynamics and immune phenotypes.

Results: Patients displayed variable lineage mosaicism correlating with two predominant clinical outcomes: early-onset severe atopy with hypereosinophilia, and autoimmune-lymphoproliferative immunodeficiency with expansions of CD8 and γδ T cells. Functional studies revealed enhanced IL-2–mediated proliferation, effector differentiation, and oligoclonal T-cell expansions. In mice, a few mutant hematopoietic stem cells reproduced the patient lineage-skewed immune landscapes with variable growth advantage of mutant cells across hematopoietic development and recapitulated patient T-cell phenotypes. Targeted mTOR inhibition successfully controlled lymphoproliferation in patients.

Conclusion: A single somatic variant in a few stem cells can remodel hematopoiesis, generating variable immune mosaics and heterogeneous immune disease. (J Allergy Clin Immunol 2026;157:964-76.)

Key words: *STAT5B, somatic mosaicism, hematopoietic stem cells, clonal hematopoiesis, immune dysregulation, T-cell lymphoproliferation, autoimmunity, atopy, mTOR inhibition*

From [a]the Institute for Immunodeficiency, Center for Chronic Immunodeficiency, University Medical Center Freiburg, Faculty of Medicine, University of Freiburg, Freiburg; [b]the Faculty of Biology, University of Freiburg, Freiburg; [c]the Signalling Research Centre CIBSS, University of Freiburg, Freiburg; [d]the Institute of Animal Breeding and Genetics, University of Veterinary Medicine, Vienna; [e]the Max-Planck-Institute for Immunobiology and Epigenetics, Freiburg; [f]the Division of Stem Cell Transplantation, University Children's Hospital Zurich, Eleonore Foundation & Children's Research Center (CRC), Zurich; [g]the Center for Pediatrics and Adolescent Medicine, University Medical Center Freiburg, Faculty of Medicine, University of Freiburg, Freiburg; [h]Children's Health Ireland at Crumlin and University of Dublin, Trinity College Dublin, Dublin; [i]Montpellier University, INSERM U1183, IRMB, IHU Immu4Cure, Clinical Genetic Department, Montpellier University Hospital, Montpellier; [j]the Department of Molecular Genetics and Cytogenomics, University Hospital of Montpellier, Montpellier; [k]the University of Montpellier, INSERM U1183, IRMB, IHU Immun4Cure, French National Reference Center of Autoinflammatory Diseases and Amyloidosis (CeRéMAIA), CHU Montpellier, Department of Molecular Genetics and Cytogenomics, National Reference Laboratory of Autoinflammatory Diseases, Montpellier; [l]the University of Montpellier, Department of Respiratory Disease, PhyMedExp, INSERM U1046, CNRS UMR 9214, CHU Montpellier, Montpellier; [m]the Clinic for Internal Medicine II, Gastroenterology, Hepatology, Endocrinology, and Infectious Disease, University Medical Center Freiburg, Faculty of Medicine, University of Freiburg, Freiburg; [n]the Department of Pediatrics and Adolescent Medicine, Division of Pediatric Hematology and Oncology, University Medical Center Freiburg, Faculty of Medicine, University of Freiburg, Freiburg; [o]the Institute of Medical Bioinfomatics and Systems Medicine, University Medical Center Freiburg, Faculty of Medicine, University of Freiburg, Freiburg; [p]the German Cancer Consortium (DKTK), Partner Site Freiburg, a partnership between DKFZ and Medical Center–University of Freiburg, Freiburg; [q]the Department of Pediatrics and Adolescent Medicine, University Medical Center Ulm, Ulm; [r]the Center of Human Genetics Tübingen, Tübingen; [s]CeGaT GmbH Tübingen, Tübingen; [t]the Institute for Transfusion Medicine, University of Ulm, Ulm; [u]the Institute for Clinical Transfusion Medicine and Immunogenetics Ulm, German Red Cross Blood Service Baden-Wurttemberg—Hessen, Ulm; and [v]the Department of Biosciences & Medical Biology, Paris Lodron University Salzburg, Salzburg.

Received for publication September 9, 2025; revised November 14, 2025; accepted for publication December 1, 2025.

Available online December 24, 2025.

Corresponding author: Stephan Ehl, MD, Center for Chronic Immunodeficiency, Breisacher Str. 115, 79106 Freiburg, Germany. E-mail: stephan.ehl@uniklinik-freiburg.de.

0091-6749

https://doi.org/10.1016/j.jaci.2025.12.993

Abbreviations used
Bcl-2: B-cell lymphoma 2
BM: Bone marrow
FACS: Fluorescence-activated cell sorting
HD: Healthy donor
HSC: Hematopoietic stem cell
HSCT: HSC transplantation
JAK: Janus kinase
LSK: Lineage$^-$Sca-1$^+$c-Kit$^+$
mTOR: Mammalian target of rapamycin
NK: Natural killer
pY: Tyrosine phosphorylation
RNA-Seq: RNA sequencing
T-bet: T-box expressed in T cells
WT: Wild type

Inborn errors of immunity are traditionally linked to germline mutations in immune-related genes.[1] More recently, however, somatic mosaicism has emerged as an alternative mechanism, often leading to phenocopies of germline inborn errors of immunity.[2] Somatic mosaicism involves genetic changes present in a subset of cells and can arise from early postzygotic cells during embryonic development to mature immune cells in adulthood. Like germline variants, somatic mutations can alter activity of immune-related proteins, leading to aberrant immune cell function and disease.

The pathophysiologic consequences of a somatic mutation—from the initial mutation in a single cell to its effect on larger immune cell populations and disease—must be decoded for each gene separately. Among the more than 20 genetic errors of immunity with somatic mosaicism described so far, most conditions can be explained by an early postzygotic somatic event.[3] Here, the mutation is present in a fraction of all somatic or all hematopoietic cells without the need for a proliferative advantage of mutant cells. In a few exceptions, the initiating mutation is acquired at a later developmental stage in a hematopoietic stem cell (HSC).[4-6] In these cases, the mutation must confer a significant growth advantage to eventually cause relevant mosaicism in the immune system. Depending on the affected gene and the resulting pathophysiology, the variant allele frequency in different immune cell types can vary significantly. For example, somatic *FAS* mutations are enriched in double-negative T cells, but they are rare in hematopoietic progenitors.[4] In contrast, *UBA1* mutations are largely restricted to myeloid cells as a result of impaired survival of mutant lymphoid progenitors.[6] At the stem cell level, inflammation caused by *UBA1* mutations disrupts normal hematopoiesis and drives clonal dominance.[7] Understanding lineage-specific clonal dynamics conferred by these genetic variants is crucial for improving diagnostic and prognostic tools and therapy.

Recently the somatic *STAT5B*^{N642H} variant has been identified in 3 children with severe early-onset atopy.[8-10] This was unexpected because the *STAT5B*^{N642H} variant is a known driver in T-cell, natural killer (NK) cell, and eosinophil malignancies.[11-15] It confers gain-of-function activity by stabilizing a hyperactive protein conformation, increasing transcriptional activity, accelerating cell cycle progression, and increasing resistance to apoptosis.[14-17] STAT5B signaling in response to various cytokines—including IL-2, IL-3, IL-5, IL-7, IL-9, IL-11, and IL-15 as well as granulocyte-macrophage colony-stimulating factor—regulates the development, differentiation, proliferation, and survival of multiple hematopoietic and immune cell types, including T cells, NK cells, and eosinophils.[14-17] In previously reported patients, the mutation was found in all hematopoietic lineages, leaving open whether disease originated from early postzygotic events or later HSC mutations conferring proliferative advantage. Moreover, the functional consequences of *STAT5B*^{N642H} in nonmalignant human immune cells remain poorly defined.

Here we expand the phenotypic spectrum of somatic *STAT5B*^{N642H}-associated disease by describing autoimmune lymphoproliferative disease in the absence of atopy in two patients, including one with late-onset presentation. Restriction of the mutation to NK and T cells supports the concept that acquisition in a single hematopoetic progenitor may suffice to cause disease. To model this, we generated mice with mosaic *STAT5B*^{N642H} expression in a few HSCs. This system confirmed that selective advantage across hematopoietic subsets drives lineage-specific mosaicism creating diverse immune landscapes, resulting in diverse immune-mediated diseases.

METHODS

Patients and mice

Patients were recruited to this study after receipt of their informed consent (approval 409/16). Mouse experiments were approved by the Regierungspräsidium Freiburg (G-21/090). Wild-type (WT) C57BL/6 Ly5.1/CD45.1 mice were purchased from Charles River Laboratories. Bones of *hSTAT5B*^{N642H} transgenic (B6N-Tg(STAT5BN/H)726Biat female mice were obtained from Richard Moriggl, Vienna.[14] Mice were housed under specific pathogen–free conditions. More information about the generation of bone marrow (BM) chimeras is available in the Methods section in the Online Repository available at www.jacionline.org.

Flow cytometry

Blood samples of patient 5 were obtained and frozen before any immunosuppressive therapy was administered. Patient 6 underwent sampling 1 month after he had stopped a 6-month course of ruxolitinib and while he was receiving 5 mg decortin and 2 mg rapamycin. We thawed and analyzed the samples of patients 5 and 6 and respective controls on the same day to avoid variations in flow cytometry. Staining details, antibodies, and functional immunologic assays including immunoblotting are provided in the Methods section in the Online Repository.

Mass cytometry

Mass cytometry reagents were commercially obtained or generated by custom conjugation to isotope-loaded polymers using MAXPAR kit (Fluidigm). Single-cell suspensions were pelleted, incubated with 20 μmol lanthanum-139 (Trace Sciences)-loaded maleimido-mono-amine-DOTA (Macrocyclics) in phosphate-buffered saline for 5 minutes at room temperature. A β_2-microglobulin–based barcoding approach was used to minimize batch effects.[18] More details are provided in the Methods section in the Online Repository.

TABLE I. Clinical summary of patients with somatic *STAT5B*^{N642H} mosaicism

Characteristic	Patient 1	Patient 2	Patient 3	Patient 4	Patient 5	Patient 6
Age at onset	4 mo	1 wk	3 mo	6 wk	6 wk	10 y
Age at last observation	12 y	2 y (died after HSCT)	4 y	12 y (HSCT at age 3 y)	9 y	54 y
Atopic manifestations	Urticaria, AD, angioedema	Urticaria, AD, food allergies, eosGE	Urticaria, AD, food allergies, eosGE	Urticaria, AD, angioedema	None	None*
Peak eosinophilia (/μL)	6,600	77,000	22,000	30,000	11,800	240
Peak IgE (U/mL)	<20	>6,000	4,385	201	1	9
Lymphoproliferation	SM		HSM, LAP	HSM, LAP	HSM, LAP	SM (25 y), LAP (35 y)
Autoimmunity/ immunodeficiency	Alopecia, chronic diarrhea	Panniculitis, bronchiolitis	Chronic diarrhea	Alopecia	Type 1 diabetes, hypogammaglobulinemia	Inflammatory (neutrophilic) skin and lung disease*†
T-cell counts		NA	NA			
Age	10 y			6 mo	2.8 y	54 y
CD4 (/μL)	1,225 n			10,200 ↑	2,173 n	1,684 n
CD8 (/μL)	1,806 ↑			6,210 ↑	9,534 ↑	4,748 ↑
γδ (/μL)	432 ↑			2,020 ↑	1,783 ↑	NA

For patients 1, 2, and 3, data have been previously reported elsewhere, and information was extracted from indicated references, with current update provided for patient 1. Patient 1 data are from Eisenberg et al,[9] Ma et al,[8] and this study. Patient 2 data are from Ma et al.[8] Patient 3 data are from Eisenberg et al[9] and Kobets et al.[10] Data for patients 4, 5, and 6 are from this study. Reference value for eosinophils is <500/μL and for IgE is <20 U/mL.

AD, Atopic dermatitis; *EosGE,* eosinophilic gastroenteritis; *HSM,* hepatosplenomegaly; *LAP,* lymphadenopathy; *n,* normal; *NA,* not applicable; *SM,* splenomegaly.

*Patient had severe chronic obstructive inflammatory lung disease, which was initially diagnosed as asthma, but which was unresponsive to conventional antiasthma therapy and not accompanied by elevated IgE, eosinophilia, or demonstrable allergic sensitization.

†Patient spent his childhood in Africa (Congo) and experienced a large number of tropical infectious diseases including malaria, amebiasis, lambliasis, and suspected schistosomiasis. He also had fungal skin infections and *Mycobacterium avium* infection of lung.

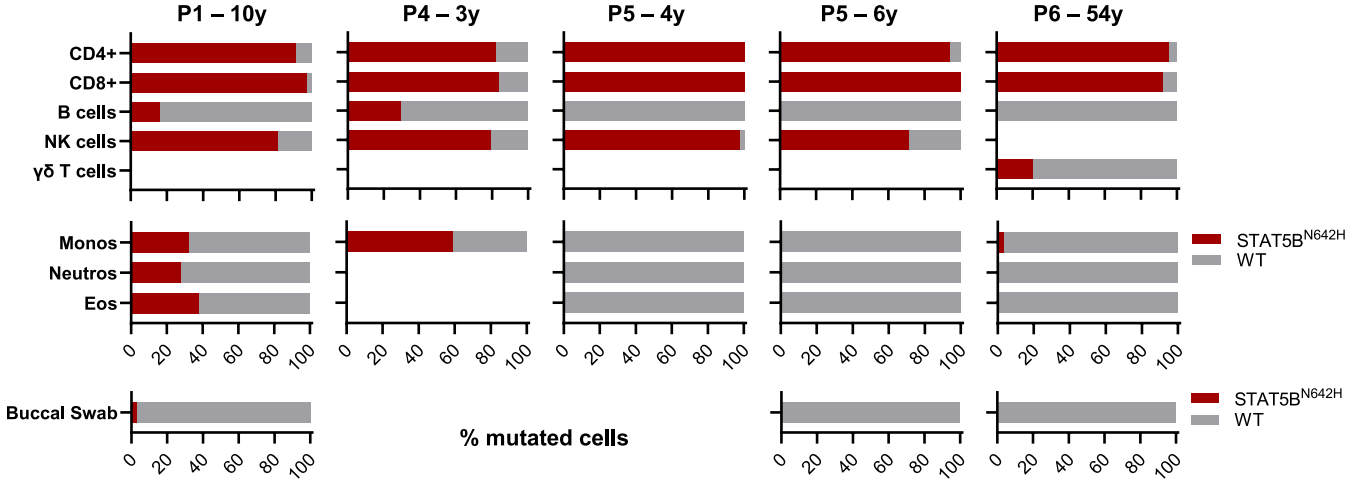

FIG 1. Lineage distribution of *STAT5B*^{N642H} mosaicism. Indicated cell populations were sorted from peripheral blood, and allele frequency of *STAT5B*^{N642H} was determined by deep sequencing (>600-fold). Buccal swab DNA was analyzed from patient 1 (P1), P5, and P6. *Red bars* show fraction of mutant cells assuming heterozygosity.

Sequencing

Cell population–specific genetic analysis of *STAT5B* was performed after isolating DNA from sorted cell populations. To determine relative *STAT5B* allele frequencies, in initial experiments, the area under the peak was obtained by Mutation Surveyor software (Softgenetics). Results were confirmed in all patients by next-generation sequencing. For bulk RNA sequencing (RNA-Seq), the mRNA from CD8 T cells sorted by fluorescence-activated cell sorting (FACS) was isolated with a RNeasy Micro Kit (Qiagen, 74004). Library preparation and analysis are described in detail in the Methods section in the Online Repository. For TCR β CDR3 sequencing, DNA of FACS-sorted CD8 T cells was purified with a QIAamp DNA Blood Mini Kit (Qiagen, 51104), and the TCR β chain CDR3 region was sequenced with an immunoSEQ Assay. Total and productive unique sequences were analyzed by the ImmunoSEQ Analyzer (Adaptive Biotechnologies).

Statistical analysis

Statistical analyses were performed by GraphPad Prism v9 software (GraphPad Software). Statistical tests are reported in the

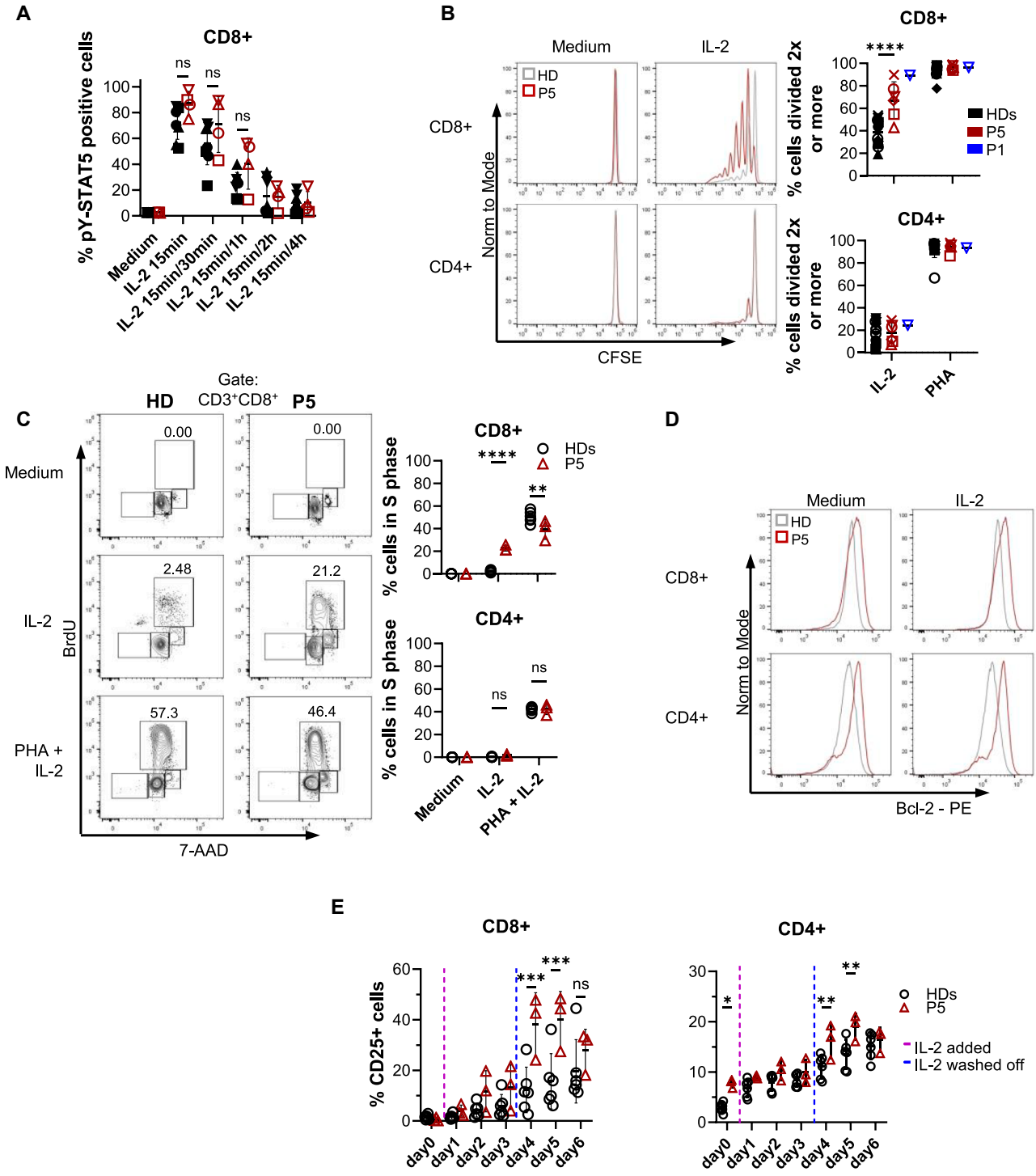

FIG 2. *STAT5B*^{N642H} promotes CD8 T-cell proliferation by increasing responsiveness to IL-2 and BCL2 expression. **(A)** Flow cytometry analysis of pY-STAT5 in primary CD8 and CD4 T cells of patient 5 (P5) (n = 4) and HDs (n = 8) stimulated with 15 ng/mL IL-2 for 15 minutes, washed, and rested for indicated time periods (4 independent experiments). **(B)** Histograms and summary plots of proliferation of primary T cells of P1 (n = 1), P5 (n = 7), and HDs (n = 14) after stimulation with 7.5 ng/mL IL-2 or 2.5 μg/mL PHA for 7 days using CFSE dilution (analyzed in 7 independent experiments). **(C)** Contour and summary plots of cell cycle analysis of primary CD4 and CD8 T cells of P5 (n = 3) and HDs (n = 6) stimulated with 15 ng/mL IL-2 alone or PHA and IL-2 (2.5 μg/mL, 1.5 ng/mL) for 3 days (3 independent experiments). **(D)** Bcl-2 expression in primary CD4 or CD8 T cells at baseline and after 15 ng/mL IL-2 stimulation for 16 hours. **(E)** Daily analysis of CD25 expression on primary CD4 or CD8 T cells from P5 (n = 3) and HDs (n = 6) at baseline, during 3 days of culture with 15 ng/mL IL-2, and after washing and IL-2 starving for 3 days (3 independent experiments). Statistical analysis by Šídák multiple comparisons test. *CFSE,* Carboxyfluorescein succinimidyl ester; *PHA,* phytohemagglutinin.

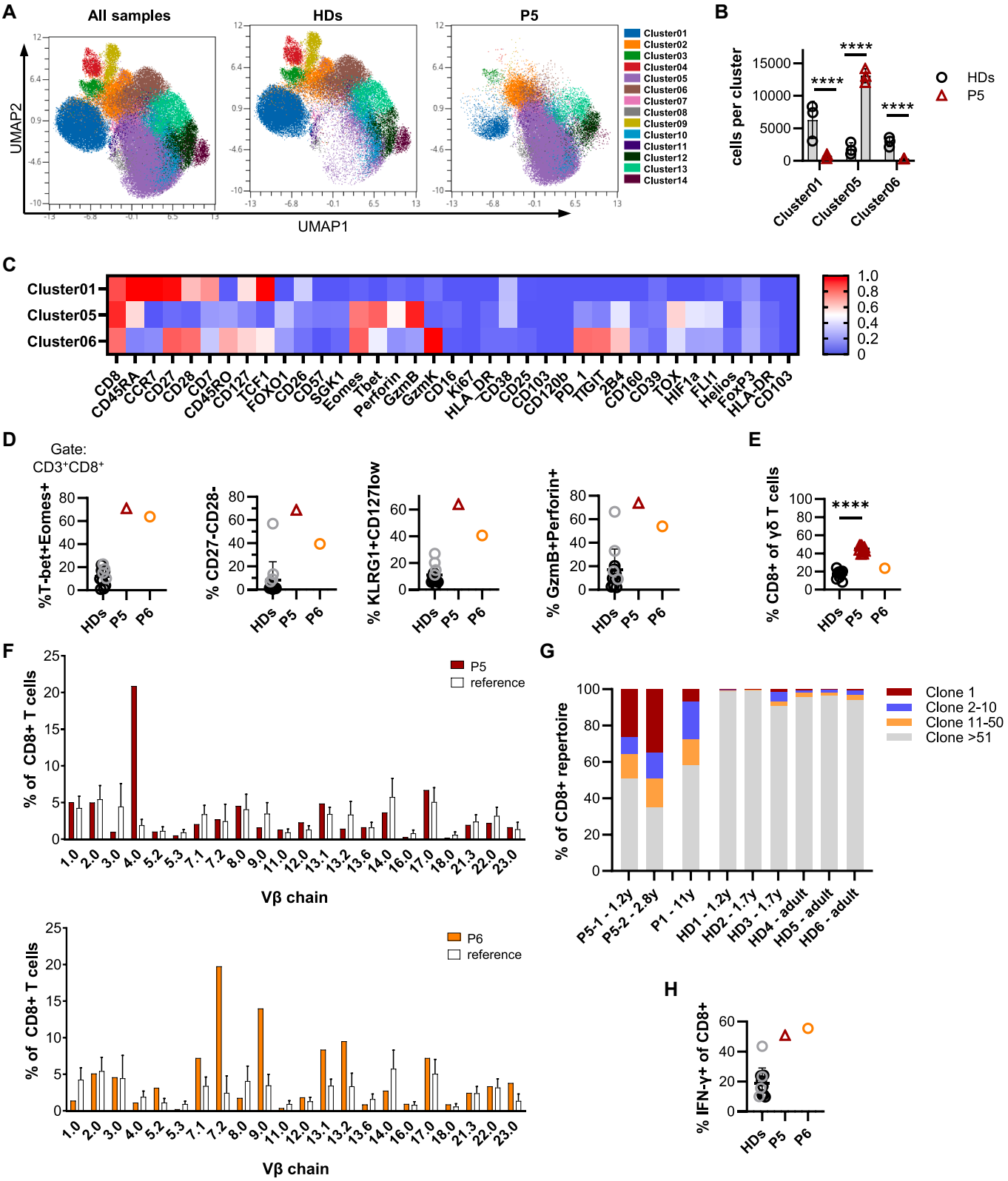

FIG 3. *STAT5B*^{N642H} alters differentiation and clonality of CD8 T cells. **(A)** Mass cytometry UMAP visualization and FlowSOM clustering of CD8 T cells from HDs (n = 3) and patient 5 (P5; n = 3, samples from different time points) downsampled to 17.867 cells for each individual. **(B)** CD8 T-cell clusters with significant numeric differences between P5 and HDs. **(C)** Heat map of min-max–normalized marker expression of selected clusters. **(D)** Expression of selected CD8 T-cell differentiation markers on PBMCs as determined by flow cytometry (age-matched HDs for P5, *solid circles,* n = 8; for P6, *open circles,* n = 6). **(E)** Percentage

figures, with asterisks indicating corresponding significance (*$P < .05$, **$P < .01$, ***$P < .001$, ****$P < .0001$).

RESULTS

Somatic *STAT5B*^{N642H} mosaicism associated with atopic and/or autoimmune-lymphoproliferative phenotypes

We identified 3 previously unreported patients with somatic *STAT5B*^{N642H} mosaicism (Table I). Patient 4 sought care at 2 months with severe dermatitis, angioedema, urticaria, hypereosinophilia, lymphadenopathy, and splenomegaly. At 2 years, he experienced cerebral ischemic events attributed to eosinophilic syndrome, prompting HSC transplantation (HSCT) at age 3. Despite initial remission, moderate eosinophilia recurred 6 years later and persists (now age 12). Patient 5 presented at 6 weeks with lymphadenopathy and hepatosplenomegaly. He had transient infantile eosinophilia but never showed allergic symptoms. He developed hypogammaglobulinemia requiring immunoglobulin substitution, and type 1 diabetes at 10 months. Rapamycin fully controlled his lymphoproliferation, he remains well at age 10. Patient 6, a 54-year-old man, was referred in 2018 for chronic inflammatory skin and lung disease, splenomegaly, and lymphadenopathy. His childhood in Africa was notable for multiple tropical infections. At 10 years, he developed obstructive lung disease unresponsive to standard therapy and not accompanied by elevated IgE, eosinophilia, or allergic sensitization. Lymphoproliferation emerged in his 20s. By 2018, he had chronic obstructive pulmonary disease with bronchiectasis and neutrophilic inflammation, revealed by biopsy. Eosinophils and immunoglobulins including IgE were normal. Steroids improved symptoms, while steroid-sparing biologics provided limited benefit; rapamycin improved lung function. All 3 patients showed CD8 T-cell lymphocytosis, with concurrent γδ T-cell lymphocytosis in patients 4 and 5 (Table I).

Previously reported cases (patients 1, 2, and 3) are summarized in Table I.[8-10] Patient 1 sought care at 4 months with annular erythema and urticaria,[8,9] later developing dermatitis, alopecia, angioedema, arthralgias, and diarrhea that were partially responsive to ruxolitinib (now age 13). Patient 2[8] and patient 3[9,10] also had severe infantile atopy. Patient 2 additionally developed panniculitis and bronchiolitis and died after HSCT at age 2, while patient 3 (reported until age 4) exhibited lymphoproliferation and diarrhea.

Lineage distribution of *STAT5B*^{N642H} mosaicism correlates with clinical phenotype

Whole-exome sequencing in the 3 new patients identified *STAT5B*^{N642H} with variant allele frequencies of 20% to 30% as the sole pathogenic finding. In patient 4, retrospective analysis of pre-HSCT samples established the diagnosis. The distribution of *STAT5B*^{N642H}-mutant cells determined by next-generation sequencing of FACS-sorted populations is depicted in Fig 1, incorporating follow-up data from patient 1 and longitudinal data from patient 5. Across patients, 80% to 100% of T and NK cells carried the variant, and 20% of γδ T cells in patient 6. In patients with predominant primary allergic disease (patients 1 and 4, Fig 1), the variant appeared in 20% to 40% of B cells, eosinophils, and other myeloid cells, consistent with reports from patients 1, 2, and 3.[8,9] In contrast, patients with an autoimmune-lymphoproliferative phenotype (patients 5 and 6, Fig 1) lacked detectable variants in B cells, myeloid cells, and buccal swabs.

STAT5B^{N642H} enhances IL-2–induced proliferation in patient CD8 T cells

We investigated the functional impact of *STAT5B*^{N642H} on primary and *in vitro*–expanded T cells. Unlike cell lines overexpressing *STAT5B*^{N642H} or T cells from *STAT5B*^{N642H} mice,[14-16] patient 5's T cells showed no higher STAT5 baseline tyrosine phosphorylation (pY) and only slightly increased pY-STAT5 after IL-2 stimulation in CD8 T cells (Fig 2, *A*). Nevertheless, CD8, but not CD4, T cells exhibited increased proliferation (Fig 2, *B*) and enhanced cell cycle entry (Fig 2, *C*) after IL-2 stimulation. The STAT5 target B-cell lymphoma 2 (Bcl-2)[19] was elevated in patient 5's T cells *ex vivo* and after IL-2 stimulation (Fig 2, *D*). CD25, another STAT5 target,[19] was similarly expressed in resting patient and healthy donor (HD) T cells, but it increased to higher levels in patient T cells after IL-2 withdrawal, a condition disrupting IL-2 receptor recycling (Fig 2, *E*).[20] Thus, *STAT5B*^{N642H} confers a proliferative advantage to CD8 T cells via a positive feedback loop of increased IL-2 responsiveness driving enhanced CD25 and Bcl-2 expression.

STAT5B^{N642H} drives effector T-cell differentiation and oligoclonal expansion

Mass cytometry of peripheral blood mononuclear cells from patient 5, sampled over 3 years, revealed marked disparities in CD8$^+$ T-cell subsets compared to HDs (Fig 3, *A;* the gating strategy is provided in Fig E1, *A,* in the Online Repository available at www.jacionline.org). Patient 5 exhibited a striking accumulation of terminally differentiated cytotoxic memory CD8$^+$ T cells (cluster 5) with reduced naive (cluster 1) and "exhausted-like" (cluster 6) subsets (Fig 3, *B*). Cluster 5 was defined by CD45RA expression, low-to-negative CCR7, CD127, CD27, and CD28 levels, and high CD38, CD39, and CD57. Coexpression of T-box expressed in T cells (T-bet) and Eomesodermin (EOMES) correlated with strong Perforin and Granzyme B expression (Fig 3, *C;* full cluster heat map in Fig E1, *B*). Reduction of clusters 4 and 9 was highly variable in controls and not significant.

Flow cytometry confirmed these findings in patients 5 and 6 (Fig 3, *D*). Over 40% of expanded γδ T cells expressed CD8 (Fig 3, *E*). Both patients demonstrated oligoclonal CD8 T-cell

of γδ T cells expressing CD8 in P5 (6 separate analyses), P6, and age-matched donors. **(F)** Vβ repertoire analysis of CD8 T cells as determined by flow cytometry. Reference range was determined in group of 32 healthy young adults. **(G)** Frequency of top expanded TCR β sequences of CD8 T cells of P1 and P5 compared to age-matched and adult HDs (n = 3 each) as determined by TCR β deep sequencing. Clone 1 in 2 samples of P5 represents identical sequence. Colors represent clone rank, not specific clone sequence. **(H)** IFN-γ production by CD8 T cells after 4 hours' PMA/ionomycin stimulation. Statistical analysis by Šídák multiple comparisons test (*A* and *E*). *PMA,* Phorbol 12-myristate 13-acetate; *PBMC,* peripheral blood mononuclear cell; *UMAP,* uniform manifold approximation and projection.

expansions as assessed by flow cytometric analysis of Vβ chain usage (Fig 3, *F*). Notably, in patient 5 the CD8 phenotype was not restricted to the expanded Vβ4$^+$ cells but was also observed in Vβ4$^-$ cells (Fig E1, *C*). TCR β CDR3 sequencing was performed from sorted CD8 T cells from patients 1 and 5 (Fig 3, *G*). The 10 most prevalent TCR β CDR3 sequences comprised 36% of the total repertoire in patient 5, expanding to 47% over follow-up, and 27% in patient 1 compared to <5% in age-matched and adult controls. CD8 T cells from patients 5 and 6 demonstrated elevated intracellular IFN-γ on stimulation (Fig 3, *H*).

Also, among CD4 T cells, T-bet/Eomesodermin double-positive, CD27$^-$CD28$^-$, CD127$^-$KLRG1$^+$, and Granzyme B$^+$ and Perforin$^+$ cytotoxic memory cells were expanded (see Fig E2, *A-D,* as well as the gating strategy and full heatmap in Fig E3, both in the Online Repository available at www.jacionline.org). IFN-γ producing CD4 T cells were elevated, whereas IL-4 and IL-17 producers were normal (Fig E2, *E*). Regulatory T cells were normal to increased, and T follicular helper cells were reduced (Fig E2, *F*). Vβ repertoire analysis showed Vβ11$^+$ CD4 T-cell expansion in patient 5 and multiple oligoclonal T-cell expansions in patient 6 (Fig E2, *G*). Collectively, *STAT5B*^{N642H} promoted effector memory differentiation, altered T helper cell balance differentiation,[8-10] influenced oligoclonal T-cell expansions, and induced accumulation of γδ T cells expressing CD8. NK cells in patient 5—with 60% carrying the mutation—showed normal counts, cytotoxic function, and cytokine production (see Fig E4 in the Online Repository).

STAT5B^{N642H} conveys variable growth advantage to different leukocyte populations

Restriction of the genetic variant to NK and T cells in two patients argued against an early postzygotic origin of mosaicism. To test whether *STAT5B*^{N642H} in a few stem cells can drive multilineage mosaicism, we generated mixed BM chimeras using transgenic mice expressing human *STAT5B*^{N642H} (*hSTAT5B*^{N642H}) under the *Vav1* promoter (Fig 4, *A*).[14] WT CD45.1 Lineage$^-$Sca-1$^+$c-Kit$^+$ (LSKs) cells were mixed 200:1 with *hSTAT5B*^{N642H} transgenic LSK cells (CD45.2), and 10,000 to 15,000 LSK cells were transplanted into conditioned CD45.1 WT recipients (WT/N642H). Mosaicism was analyzed in 2 separate experiments with 4 mice each (mice 1-8) from 6 to 12 weeks after transplantation. In mouse 6 and mouse 8, mutant cells exceeded 5% of CD4 and CD8 T cells by week 6 and >80% to 90% (CD4) by week 12. In mice 1-5, T-cell mosaicism increased later, reaching 10% to 80% by week 12. In mice 4-6 and mouse 8, mutant NK and B cells also expanded (Fig 4, *B;* for gating, see Fig E5 in the Online Repository available at www.jacionline.org). Myeloid mosaicism was less pronounced (Fig 4, *C*): mouse 6 had 40% in monocytes, neutrophils, and eosinophils; mice 4, 5, and 8 had 5% to 20%, and mice 1-3 and mouse 7 had only a few mutant myeloid cells. Overall, mice 1-3 resembled patients 5 and 6 (Fig 4, *D*), while mice 4-6 and mouse 8 mirrored patients 1 to 4. Thus, a few mutant LSK cells conferred variable developmental advantages across lineages, leading to a mosaic mutational landscape that was similar to our patients. The resulting peripheral T-cell lymphocytosis, most pronounced for CD8$^+$ αβ and γδ T cells (Fig 4, *E*), was associated with variable splenomegaly, as in our patients (Fig 4, *F*). Aside from splenomegaly, the mice showed no obvious clinical illness or eosinophilia.

Variable growth advantage of *STAT5B*^{N642H}-expressing hematopoietic precursors in different lineage trajectories

To assess growth advantage along hematopoietic differentiation, we analyzed mosaicism among various hematopoietic precursors, thymocytes, and peripheral T cells 12 weeks after HSCT. Mutant cells comprised 10% to 80% of HSCs in mice 3-6 and mouse 8, but such cells were below detection limit in mice 1, 2, and 7. Mosaicism fluctuated during differentiation to common lymphoid precursors (Fig 5; for gating, see Fig E6 in the Online Repository available at www.jacionline.org), and in mice 3 and 5 was lost during thymocyte development. In the thymus, mutant cells reached up to 90% at the double-positive stage in mice 4, 6, and 8, while others showed little or no thymic mosaicism. Post-thymic outgrowth occurred in 7 of 8 mice, most prominently in CD8 T cells (50-95%), but also in CD4 T cells (10-90%) with memory phenotypes (Fig 5). Myeloid mosaicism was detected in mice 3-6 and mouse 8, decreasing between multipotent progenitor 2 and granulocyte-macrophage progenitors, resulting in 3% to 30% mosaicism in 4 of 8 mice at week 12. Although this model does not replicate spontaneous mutation acquisition, these data show that a transgenic *STAT5B*^{N642H} allele in few stem cells can confer proliferative advantage across lineages and establish variable mosaicism, as observed in the patients.

STAT5B^{N642H} T cells in chimeric mice mimic patient T-cell phenotype

We used the chimeric mice we had generated to determine the intrinsic effects of *STAT5B*^{N642H} on T-cell differentiation by comparing mutant (CD45.2) to WT (CD45.1) cells in the same mouse. *hSTAT5B*^{N642H} CD8 T cells were enriched for memory cells (Fig 6, *A*) with downregulated CD127 (Fig 6, *B*), upregulated granzyme B (Fig 6, *C*) and coexpression of T-bet and eomesodermin (Fig 6, *D*), and they produced more IFN-γ (Fig 6, *E*), mirroring changes in patients 5 and 6. Furthermore, a higher fraction of γδ T cells expressed CD8 (Fig 6, *F*). RNA-Seq of sorted patient 5 CD8 T cells showed strong enrichment of the top 100 transcripts upregulated in CD8 T cells of *hSTAT5B*^{N642H} transgenic mice (Fig 6, *G*).[14] Mutant CD4 T cells also showed enhanced effector differentiation and a larger regulatory T-cell proportion (see Fig E7 in the Online Repository available at www.jacionline.org). These results suggest that cell-intrinsic effects of *hSTAT5B*^{N642H} are essential for driving the observed T-cell phenotype.

Signaling blockade controls excessive proliferation of patient *STAT5B*^{N642H} T cells *in vitro* and *in vivo*

RNA-Seq analysis of patient 5 CD8 T cells identified DNA repair and phosphatidylinositol 3-kinase (PI3K)/protein kinase B/mammalian target of rapamycin (mTOR) signaling as the top enriched pathways compared to HDs (Fig 7, *A*). We therefore performed IL-2–mediated stimulation experiments to determine the doses at which the mTOR inhibitor rapamycin and the Janus kinase (JAK) 1/2 inhibitor ruxolitinib *in vitro* caused an identical mild inhibition of HD CD8 T-cell proliferation (Fig 7, *B*). At these doses, rapamycin more effectively controlled the hyperproliferation of mutant T cells than ruxolitinib (Fig 7, *C* and *D*). Considering these findings and good tolerance, we treated patient 5 with rapamycin and saw complete remission of splenomegaly within 3 months and a drop of CD8 T-cell counts (Fig 7, *E*).

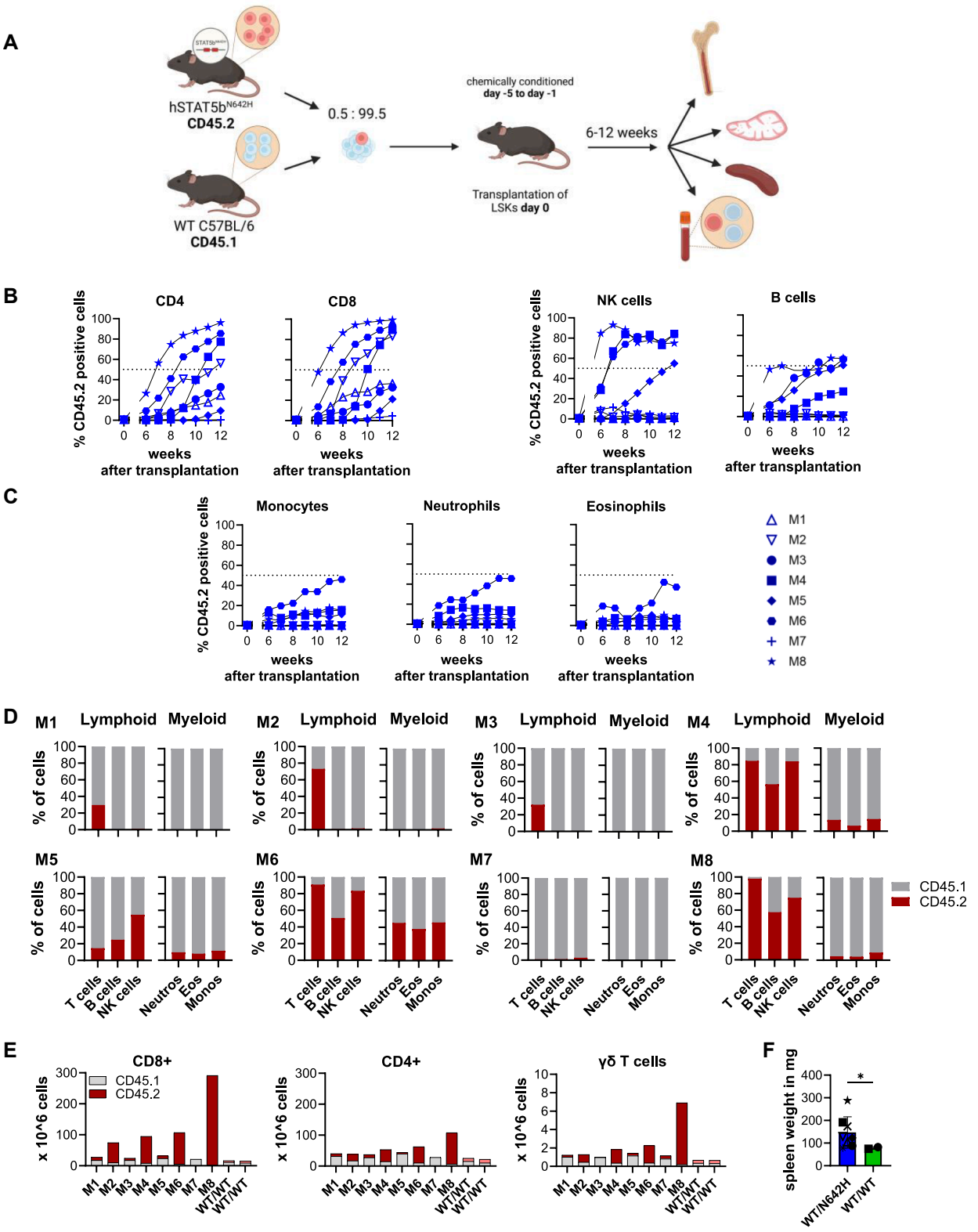

FIG 4. *STAT5B*^{N642H} chimeric mice show variable lineage distribution of *STAT5B*^{N642H} mosaicism among mature leukocytes. **(A)** Experimental setup to generate *STAT5B*^{N642H} chimeras. Image created by BioRender.com. Mutant LSK cells were transplanted at ratio of 1:200 relative to WT cells. **(B)** Proportion of CD45.2 (*STAT5B*^{N642H}) lymphoid cells in blood from week 6 to week 12 after LSK cell transplantation. Each mouse (n = 8, pooled from 2 independent experiments) is depicted with unique symbol. **(C)** Proportion of CD45.2 (*STAT5B*^{N642H}) myeloid cells in blood. **(D)** Proportion of CD45.1 (WT, *gray*) and CD45.2 (*STAT5B*^{N642H}, *red*) lymphoid and myeloid cells in blood at 12 weeks after transplantation. **(E)** Cell counts of splenic CD45.1 (WT) and CD45.2 (*STAT5B*^{N642H}) CD8, CD4, and γδ T cells. **(F)** Spleen weight. Statistical analysis by Welch *t* test.

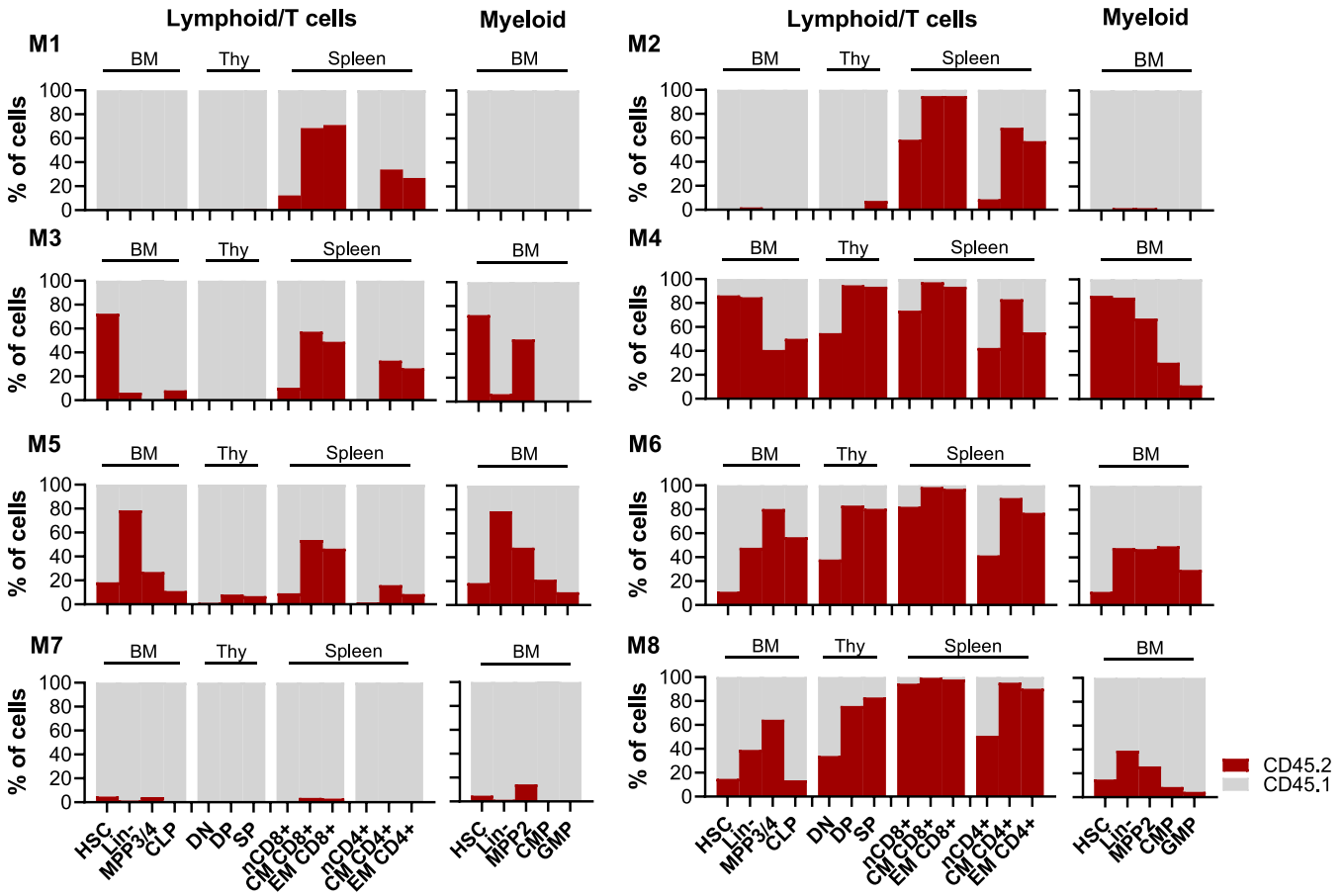

FIG 5. *STAT5B*^{N642H} chimeric mice show variable mutation distribution among hematopoietic precursors. Proportion of CD45.1 (WT, *gray*) and CD45.2 (*STAT5B*^{N642H}, *red*) lymphoid and myeloid cells in indicated developmental stages from BM to spleen as determined at week 12 after transplantation. Each mouse (M1 to M8) is depicted separately. *CLP,* Common lymphoid progenitor; *CM,* central memory; *CMP,* common myeloid progenitor; *DN,* double negative; *DP,* double positive; *EM,* effector memory; *GMP,* granulocyte macrophage progenitor); *MPP,* multipotent progenitor; *n,* naive; *SP,* single positive; *Thy,* thymus.

A transient inrease occurred during uncertain compliance, followed by stability for 3 years. The prominent CD8 Vβ4^{+} T-cell population decreased (Fig 7, *F*), though a recent rise in Vβ4^{+} CD8 T cells was observed, but without splenomegaly.

Evolution of lineage-specific mosaicism after HSCT confirms the variability of clonal dominance conferred by *STAT5B*^{N642H}

HSCT is a further treatment option for somatic *STAT5B*^{N642H}-associated disease. Patient 4 received HSCT at age 3. A first cord blood graft was rejected, followed by a haploidentical maternal graft, resulting in full donor chimerism for 3 years. Short tandem repeat analysis later showed gradual reappearance of recipient cells, beginning with CD15^{+} myeloid cells, then NK cells, B cells, and eosinophils (Fig 7, *G*). The patient developed eosinophilia, allergic eyelid swelling, and intermittent diarrhea, suggesting disease recurrence and indicating that complete donor chimerism is needed for cure. Eight years after HSCT, deep sequencing revealed altered *STAT5B*^{N642H} mosaicism across leukocyte subsets compared to pre-HSCT: T cells 80% → 0.5%, NK cells 78% → 25%, B cells 30% → 1%, and monocytes 80% → 10% (Fig 7, *H*). These results mirror our mouse experiments, showing that *STAT5B*^{N642H} in a few progenitors can produce highly variable immune landscapes even within the same host.

DISCUSSION

We show that acquisition of the activating *STAT5B*^{N642H} variant in multilineage hematopoietic precursor cells can induce variable myeloid and lymphoid mosaicism, with lineage-specific functional immune cell alterations producing a spectrum of immune dysregulation phenotypes.

STAT5B^{N642H} is a known mutation in T-cell malignancies and myeloid neoplasms, including eosinophilic disorders and acute myeloid leukemia.[11-13,17,21] Pan-hematopoietic expression in mice drives T-cell differentiation and leukemic transformation,[14,15] while NK cell–specific expression causes indolent to aggressive NK cell–large granular lymphocytic leukemia.[16] The variant enhances self-renewal, proliferation, and survival of HSCs and progenitors,[22] affecting all early hematopoietic compartments.[14] Our study clarifies that *STAT5B*^{N642H} confers a

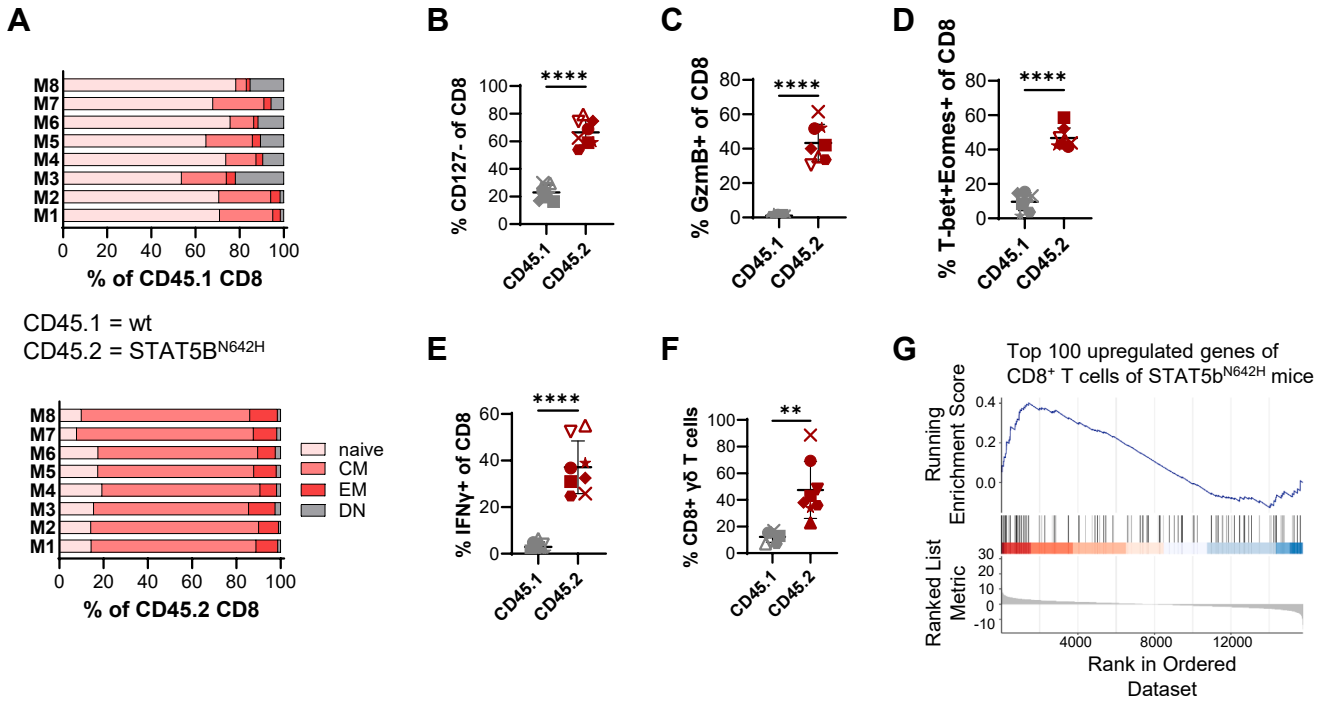

FIG 6. *STAT5B*^{N642H}-mutant CD8 T cells in chimeric mice show signature features of T cells observed in patients with somatic *STAT5B*^{N642H} variants. Chimeric mice (n = 8) generated in 2 independent experiments (as described in Fig 4, *A*) were humanely killed 12 weeks after BM transplantation, and CD45.1 (WT) and CD45.2 (*STAT5B*^{N642H}) splenic T cells were analyzed by flow cytometry. **(A)** Distribution of naive, CM, and EM CD8 T cells. **(B)** CD127 expression, **(C)** GzmB expression, and **(D)** Eomesodermin (Eomes) and T-bet expression in CD8 T cells. **(E)** IFN-γ expression of CD8 T cells after 4 hours' PMA/ionomycin stimulation. **(F)** Percentage of γδ T cells expressing CD8. **(G)** Enrichment plot showing top 100 upregulated transcripts in CD8 T cells of *STAT5B*^{N642H} mice enriched in transcriptome of patient 5 (P5) CD8 T cells (n = 3; mouse RNA-Seq data obtained from Pham et al[14]); barcode indicates position of gene in gene set rank order; *red* and *blue,* respectively, represent positive and negative Pearson correlation with CD8 T cells of P5. Statistical analysis for *(B-F)* was paired *t* test. *CM,* Central memory; *EM,* effector memory; *GzmB,* granzyme B; *PMA,* phorbol 12-myristate 13-acetate.

growth advantage to all immune cell lineages, from the BM to peripheral blood, and alters immune cell behavior to cause variable benign immune disorders.

In our patients, the mutation likely arose somatically in early hematopoietic stem/progenitor cells, supported by its presence in various blood cell lineages but its absence in buccal DNA. The early symptom onset in 5 of 6 individuals suggests *in utero* or early life acquisition, while late onset in patient 6 indicates a later event. To trace whether and how a mutation in a single precursor cell can create the observed variable genetic landscapes, we modeled this situation by transfer of mutant and WT LSK cells at a ratio of 1:200 into conditioned mice. LSK cells included both hematopoietic stem cells (HSCs) and more lineage-restricted progenitors. While all mice were transplanted from the same cell pool, cells with different lineage potential may have survived the transfer, contributing to the variable outcomes between mice. This would align with the idea that the two clinical groups of patients acquired the mutation at different progenitor levels.

It should be stated that the vav-driven *STAT5B*^{N642H} transgene does not mimic a spontaneous mutation of *STAT5B* in its natural locus, and the competitive effect starts after seeding a conditioned host, not during ongoing hematopoiesis. Despite these limitations, the competition of a few mutant hematopoetic precursor cells with a large compartment of WT cells generated a similar mosaic genetic landscape among peripheral immune cells as that observed in patients. This justified our use of the mouse model to evaluate the growth advantage of mutant cells at each stage of the hematopoietic tree, from stem cells to lineage-specific precursors, from thymocytes to mature T cells. Interestingly, we observed a range of patterns, ranging from a mostly postthymic growth advantage of T cells to pre- and intrathymic growth advantage, associated with advantages for pluripotent and more restricted lymphoid or myeloid progenitors.[23] This widespread and variable growth advantage was confirmed by patient observations. Thus, the post-HSCT mosaicism pattern in patient 4 differed from the pre-HSCT pattern, suggesting stochastic progenitor dynamics.[24] Furthermore, recurrence of mutant cells years after HSCT indicates that mutant progenitors can remain quiescent for years.[25]

A consistent finding in both patients and mice was the high proportion of mutant T cells, reflecting a postthymic growth advantage. In patient cells, IL-2–driven increased CD25 and Bcl-2 expression may underlie enhanced survival.[26] Although STAT5B phosphorylation in mature patient T cells was less pronounced than in tumor or transgenic cells,[14,16,21] mutant T cells showed altered differentiation: increased regulatory T cells, skewed T_H1/T_H2 cells, reduced T follicular helper cells, and terminally differentiated cytotoxic CD8 T cells (patients 5 and 6). These changes were

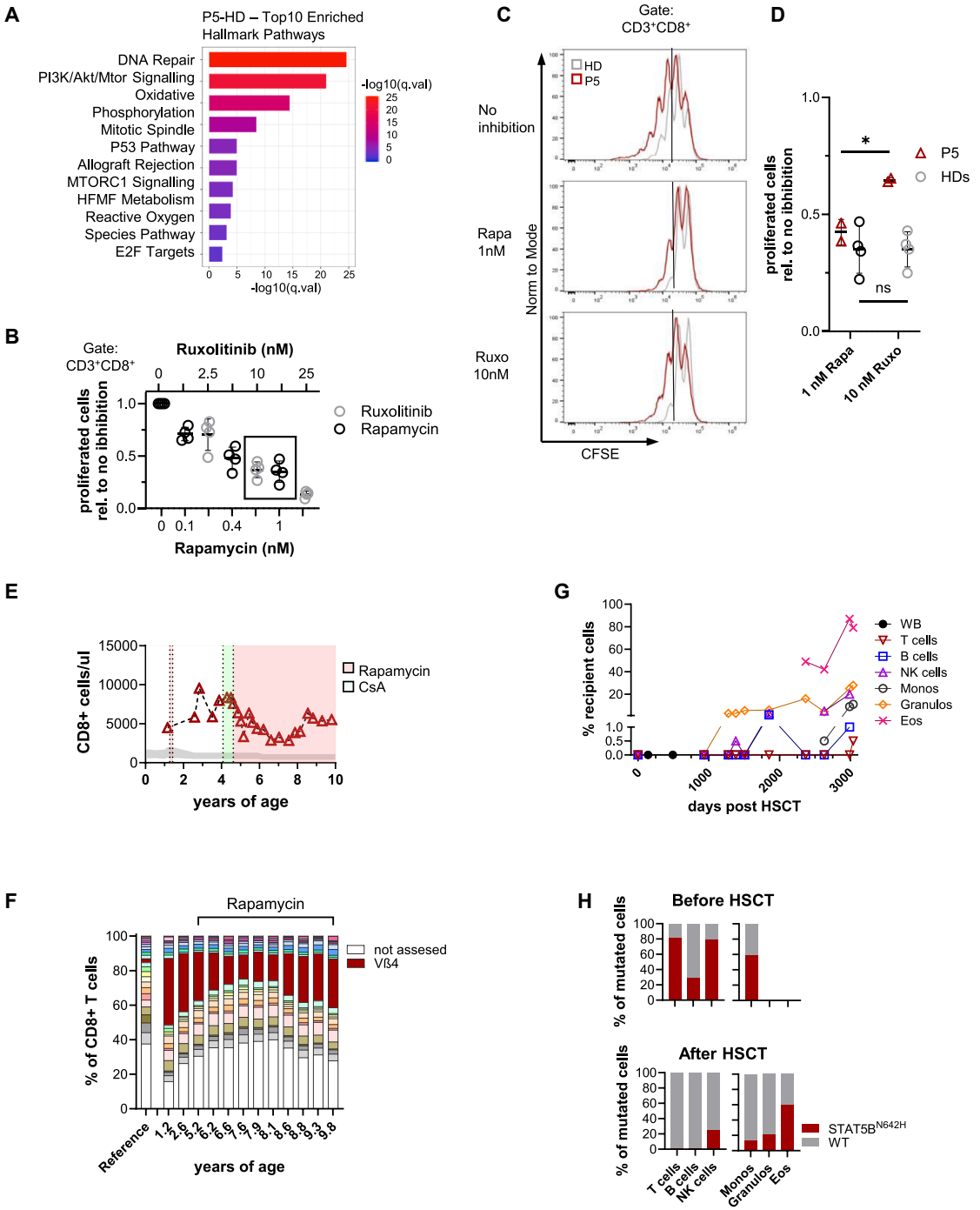

FIG 7. mTOR blockade controls *STAT5B*^{N642H}-mediated excessive T-cell proliferation. **(A)** Top 10 enriched hallmark pathways of patient 5 (P5) compared to HDs as determined by RNA-Seq of sorted CD8 T cells (HDs, n = 3; for P5, 3 samples from different time points). **(B)** Dose-finding experiment used titrated doses of rapamycin and ruxolitinib to inhibit proliferation of primary CD8 T-cell cultures of P5 (n = 2) and HDs (n = 4). CFSE dilution was determined after 7 days' 15 ng/mL IL-2 stimulation (2 independent experiments). Doses chosen for further experiments are shown in box. **(C)** CFSE dilution of HD *(gray lines)* and patient cells *(red lines)* determined at day 7. **(D)** Summary plot of proliferative response. Statistical analysis by Šídák multiple comparisons test. **(E)** Evolution of CD8 T-cell counts of P5. Treatment periods with rapamycin and CsA are depicted in *pink* and *green,* respectively. **(F)** Evolution of Vβ repertoire after treatment with rapamycin. Each color represents one Vβ family. **(G)** Progression of recipient cell chimerism after HSCT of P4 as determined by PCR of short tandem repeats in sorted blood cells. **(H)** Lineage-specific *STAT5B*^{N642H} mosaicism in peripheral blood of P4 before and 10 years after HSCT as determined by deep sequencing (>600-fold coverage) of sorted cell populations. *CFSE,* Carboxyfluorescein succinimidyl ester; *CsA,* cyclosporin.

mirrored in the chimeric mouse model at both the transcriptome and protein levels, linking *STAT5B*^{N642H} to these T-cell alterations. Despite proliferative advantage, the mutant T cells reached homeostasis without progressing to malignancy. Oligoclonal T-cell repertoires in patients, but not in mice, suggest external modifiers of the immune disease such as infections, rather than only intrinsic effects of the mutation. Importantly, oligoclonality did not evolve into malignancy over 8 to 44 years after onset of symptoms. Thus, while *STAT5B*^{N642H} clearly can be a cancer driver in certain contexts,[11,12,14-16,27] this variant alone does not always cause malignant transformation in humans.

STAT5B^{N642H} also provided a growth advantage for γδ T cells, particularly expansion of the CD8^{+} subset, which has been previously described in *STAT5B*^{N642H} transgenic mice.[28] It is still debated whether these CD8-expressing γδ T cells represent a separate lineage with specific functional properties. Despite the presence of the mutation in a significant fraction of NK cells, no abnormal expansion of NK cells was observed in patients, suggesting that *STAT5B*^{N642H} does not confer a proliferative benefit to mature nonmalignant NK cells, aligning with findings from mice.[16] Eosinophilia was an initial manifestation of 5 of 6 patients, with a high proportion of mutant eosinophils documented in 3. Notably, eosinophilia spontaneously resolved within months in patient 5, potentially as a result of quiescence or loss of an initially mutated multipotent progenitor and its downstream myeloid progenitors, but persistence of mutant lymphoid-committed precursors.[29]

Dysregulation of immune cell differentiation and function likely drove clinical manifestations. Severe atopic disease was a prominent manifestation in some patients, but it did not affect all of them. Splenomegaly, lymphadenopathy, alopecia, panniculitis, chronic diarrhea, and early-onset diabetes in patient 5 and inflammatory lung and skin disease in patient 6 likely represent additional mutation-driven manifestations. We hypothesize that T- and NK cell–restricted mutations may drive lymphoproliferation and autoimmunity, while severe allergic phenotypes may require myeloid/B-cell involvement. Notably, *STAT5B*^{N642H} variants have also been reported in elderly hypereosinophilic patients,[13,30,31] but broader lineage-specific analyses were rarely performed. The absence of eosinophilia in our *STAT5B*^{N642H} mosaic mice may be explained by the lack of a natural environmental exposure. In addition, a number of physiologic differences between human and mouse eosinophils have been described.[32] Absence of a natural exposure to infections may also explain that apart from splenomegaly, the mice did not develop obvious additional symptoms of immune dysregulation.

Genetic and transcriptional findings informed therapy. JAK inhibitors were effective in patients 1 and 3,[9] while mTOR inhibition controlled hyperproliferation in patients 5 and 6, consistent with mTOR pathway hyperactivation. Patient 5 experienced long-term clinical remission, while patient 4's post-HSCT recurrence highlights the necessity of full donor HSC chimerism.

In conclusion, somatic *STAT5B*^{N642H} mutations in hematopoietic precursors drive broad clonal hematopoiesis across immune cell lineages and confer peripheral T-cell growth advantage, causing diverse allergic and autoimmune-lymphoproliferative phenotypes. Our findings support personalized therapies guided by genetic and functional studies. Future work should address the molecular mechanism conferring growth advantage to the individual hematopoietic lineages, using epigenomic profiling, single-cell RNA-Seq, and CRISPR (clustered regularly interspaced short palindromic repeat) screens. Mouse models allowing time-controlled activation of the mutation in different cell types could clarify how mutation timing and environmental stimuli influence mosaicism and disease expression.

DISCLOSURE STATEMENT

Funded by the Deutsche Forschungsgemeinschaft (DFG) within the CRC1160 (project ID 256073931-Z02 to M.B., -A01 to S.E. and P.A., -A03 to B.B., and -A08N to A.R.E.), CRC/TRR167 (project ID 259373024-Z01 to M.B.), CRC1453 (project ID 431984000-S1 to M.B.), CRC1479 (project ID 441891347-S1 to M.B.), TRR359 (project ID 491676693-Z01 to M.B.), FOR5476 UcarE (project ID 493802833-P7 to M.B.), German Mass Cytometry Alliance (project ID 518316185, B.B.), a Heisenberg professorship (project ID 520992132 to B.B.) and CIBSS (project ID 390939984 to B.B., N.C.-W., and S.E.). Funding was also received from the German Federal Ministry of Education and Research (BMBF) within the Medical Informatics Funding Scheme (PM4Onco-FKZ 01ZZ2322A to M.B. and EkoEstMed-FKZ 01ZZ2015 to G.A).

Declaration of generative AI and AI-assisted technologies in the writing process: During the preparation of this report, the authors used Perplexity for brainstorming the discussion and ChatGPT for language editing. After using this tool/service, the authors reviewed and edited the content as needed and take full responsibility for the content of the publication.

Disclosure of potential conflict of interest: L. Heller and B. Schulte are employed by Zentrum für Humangenetik, Tübingen. B. Bengsch is on the advisory board of Roche and has received honoraria from Roivant and AstraZeneca, all unrelated to this report. The rest of the authors declare that they have no relevant conflicts of interest.

We thank the patients and their families for their trust. We thank Thomas Boehm for critical reading of the report. We thank the FREEZE biobank and the Lighthouse Core Facility (funded by the Deutsche Forschungsgemeinschaft [450392965]) for their support.

Key messages

- **Somatic *STAT5B*^{N642H} mutations in few hematopoietic stem cells create variable lineage-specific mosaicism and diverse immune disease phenotypes.**
- ***STAT5B*^{N642H} confers a proliferative advantage to CD8 and γδ T cells, driving skewed differentiation and oligoclonal expansion without inevitable malignancy.**
- **Targeted therapies such as mTOR of JAK inhibition can control disease, while HSCT requires full donor chimerism for cure.**

REFERENCES

1. Poli MC, Aksentijevich I, Bousfiha AA, Cunningham-Rundles C, Hambleton S, Klein C, et al. Human inborn errors of immunity: 2024 update on the classification from the International Union of Immunological Societies Expert Committee. J Hum Immun 2025;1:e20250003.
2. Aluri J, Cooper MA. Somatic mosaicism in inborn errors of immunity: current knowledge, challenges, and future perspectives. Semin Immunol 2023;67:101761.
3. Cooper MA. Somatic mosaicism in genetic errors of immunity. J Allergy Clin Immunol 2025;155:759-67.

4. Holzelova E, Vonarbourg C, Stolzenberg MC, Arkwright PD, Selz F, Prieur AM, et al. Autoimmune lymphoproliferative syndrome with somatic Fas mutations. N Engl J Med 2004;351:1409-18.
5. Pellé O, Moreno S, Lorenz MR, Riller Q, Fuehrer M, Stolzenberg MC, et al. Combined germline and somatic human FADD mutations cause autoimmune lymphoproliferative syndrome. J Allergy Clin Immunol 2024;153:203-15.
6. Wu Z, Gao S, Gao Q, Patel BA, Groarke EM, Feng X, et al. Early activation of inflammatory pathways in *UBA1*-mutated hematopoietic stem and progenitor cells in VEXAS. Cell Rep Med 2023;4:101160.
7. Molteni R, Fiumara M, Campochiaro C, Alfieri R, Pacini G, Licari E, et al. Mechanisms of hematopoietic clonal dominance in VEXAS syndrome. Nat Med 2025; 1911-24.
8. Ma CA, Xi L, Cauff B, DeZure A, Freeman AF, Hambleton S, et al. Somatic *STAT5b* gain-of-function mutations in early onset nonclonal eosinophilia, urticaria, dermatitis, and diarrhea. Blood 2017;129:650-3.
9. Eisenberg R, Gans MD, Leahy TR, Gothe F, Perry C, Raffeld M, et al. JAK inhibition in early-onset somatic, nonclonal *STAT5B* gain-of-function disease. J Allergy Clin Immunol Pract 2021;9:1008-10.e2.
10. Kobets AJ, Ahmad S, Boyke A, Oriko D, Holland R, Eisenberg R, et al. *STAT5b* gain-of-function disease in a child with mycobacterial osteomyelitis of the skull: rare presentation of an emerging disease entity. Childs Nerv Syst 2023;39:2071-7.
11. Rajala HL, Eldfors S, Kuusanmaki H, van Adrichem AJ, Olson T, Lagstrom S, et al. Discovery of somatic *STAT5b* mutations in large granular lymphocytic leukemia. Blood 2013;121:4541-50.
12. Bandapalli OR, Schuessele S, Kunz JB, Rausch T, Stütz AM, Tal N, et al. The activating *STAT5B* N642H mutation is a common abnormality in pediatric T-cell acute lymphoblastic leukemia and confers a higher risk of relapse. Haematologica 2014; 99:e188-92.
13. Cross NCP, Hoade Y, Tapper WJ, Carreno-Tarragona G, Fanelli T, Jawhar M, et al. Recurrent activating *STAT5B* N642H mutation in myeloid neoplasms with eosinophilia. Leukemia 2019;33:415-25.
14. Pham HTT, Maurer B, Prchal-Murphy M, Grausenburger R, Grundschober E, Javaheri T, et al. *STAT5B*^{N642H} is a driver mutation for T cell neoplasia. J Clin Invest 2018;128:387-401.
15. de Araujo ED, Erdogan F, Neubauer HA, Meneksedag-Erol D, Manaswiyoungkul P, Eram MS, et al. Structural and functional consequences of the *STAT5B*^{N642H} driver mutation. Nat Commun 2019;10:2517.
16. Klein K, Kollmann S, Hiesinger A, List J, Kendler J, Klampfl T, et al. A lineage-specific *STAT5B*^{N642H} mouse model to study NK-cell leukemia. Blood 2024;143:2474-89.
17. Brachet-Botineau M, Polomski M, Neubauer HA, Juen L, Hédou D, Viaud-Massuard MC, et al. Pharmacological inhibition of oncogenic STAT3 and STAT5 signaling in hematopoietic cancers. Cancers (Basel) 2020;12:240.
18. Schulz AR, Mei HE. Surface barcoding of live PBMC for multiplexed mass cytometry. Methods Mol Biol 2019;1989:93-108.
19. Kanai T, Seki S, Jenks JA, Kohli A, Kawli T, Martin DP, et al. Identification of *STAT5A* and *STAT5B* target genes in human T cells. PLoS One 2014;9:e86790.
20. Hémar A, Subtil A, Lieb M, Morelon E, Hellio R, Dautry-Varsat A. Endocytosis of interleukin 2 receptors in human T lymphocytes: distinct intracellular localization and fate of the receptor alpha, beta, and gamma chains. J Cell Biol 1995;129:55-64.
21. Wahnschaffe L, Braun T, Timonen S, Giri AK, Schrader A, Wagle P, et al. JAK/STAT-activating genomic alterations are a hallmark of T-PLL. Cancers (Basel) 2019;11:1833.
22. Kollmann S, Grausenburger R, Klampfl T, Prchal-Murphy M, Bastl K, Pisa H, et al. A *STAT5B*-CD9 axis determines self-renewal in hematopoietic and leukemic stem cells. Blood 2021;138:2347-59.
23. Wang Z, Emmel G, Lim HS, Zhu W, Kosters A, Ghosn EEB, et al. Stromal STAT5-mediated trophic activity regulates hematopoietic niche factors. Stem Cells 2023; 41:944-57.
24. Spencer Chapman M, Wilk CM, Boettcher S, Mitchell E, Dawson K, Williams N, et al. Clonal dynamics after allogeneic haematopoietic cell transplantation. Nature 2024;926-34.
25. Trumpp A, Essers M, Wilson A. Awakening dormant haematopoietic stem cells. Nat Rev Immunol 2010;10:201-9.
26. Grayson JM, Zajac AJ, Altman JD, Ahmed R. Cutting edge: increased expression of Bcl-2 in antigen-specific memory CD8$^+$ T cells. J Immunol 2000;164:3950-4.
27. Klein K, Witalisz-Siepracka A, Maurer B, Prinz D, Heller G, Leidenfrost N, et al. *STAT5B*^{N642H} drives transformation of NKT cells: a novel mouse model for CD56$^+$ T-LGL leukemia. Leukemia 2019;33:2336-40.
28. Sumaria N, Fiala GJ, Inácio D, Curado-Avelar M, Cachucho A, Pinheiro R, et al. Perinatal thymic-derived CD8αβ-expressing γδ T cells are innate IFN-γ producers that expand in IL-7R–STAT5B-driven neoplasms. Nat Immunol 2024;25:1207-17.
29. Pei W, Feyerabend TB, Rössler J, Wang X, Postrach D, Busch K, et al. Polylox barcoding reveals haematopoietic stem cell fates realized *in vivo*. Nature 2017; 548:456-60.
30. Ding F, Wu C, Li Y, Mukherjee S, Ghosh S, Arrossi AV, et al. A case of hypereosinophilic syndrome with *STAT5b* N642H mutation. Oxf Med Case Reports 2021; 2021:omaa129.
31. Yin CC, Tam W, Walker SM, Kaur A, Ouseph MM, Xie W, et al. *STAT5B* mutations in myeloid neoplasms differ by disease subtypes but characterize a subset of chronic myeloid neoplasms with eosinophilia and/or basophilia. Haematologica 2024;109:1825-35.
32. Lee JJ, Jacobsen EA, Ochkur SI, McGarry MP, Condjella RM, Doyle AD, et al. Human versus mouse eosinophils: "that which we call an eosinophil, by any other name would stain as red.". J Allergy Clin Immunol 2012;130:572-84.